

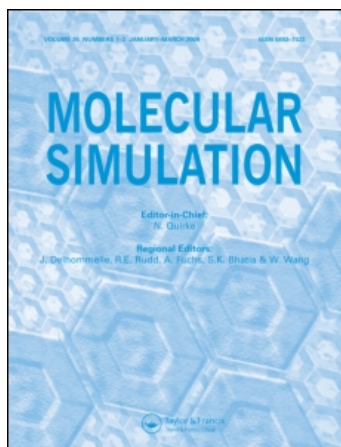
This article was downloaded by: [Esquivel, R. O.]

On: 19 April 2009

Access details: Access Details: [subscription number 910450815]

Publisher Taylor & Francis

Informa Ltd Registered in England and Wales Registered Number: 1072954 Registered office: Mortimer House, 37-41 Mortimer Street, London W1T 3JH, UK



## Molecular Simulation

Publication details, including instructions for authors and subscription information:

<http://www.informaworld.com/smpp/title-content=t713644482>

### Theoretic-information entropies analysis of nanostructures: ab initio study of PAMAM precursors and dendrimers G0 to G3

R. O. Esquivel <sup>abc</sup>; N. Flores-Gallegos <sup>c</sup>; E. M. Carrera <sup>c</sup>; J. S. Dehesa <sup>ab</sup>; J. C. Angulo <sup>ab</sup>; J. Antolín <sup>bd</sup>; C. Soriano-Correa <sup>e</sup>

<sup>a</sup> Departamento de Física Atómica, Molecular y Nuclear, Universidad de Granada, Granada, Spain <sup>b</sup> Instituto Carlos I de Física Teórica y Computacional, Universidad de Granada, Granada, Spain <sup>c</sup> Departamento de Química, Universidad Autónoma Metropolitana-Iztapalapa, Vicentina, México <sup>d</sup> Departamento de Física Aplicada, EUITIZ, Universidad de Zaragoza, Zaragoza, Spain <sup>e</sup> Laboratorio de Química Computacional, FES-Zaragoza, Universidad Nacional Autónoma de México, Iztapalapa, México

Online Publication Date: 01 May 2009

**To cite this Article** Esquivel, R. O., Flores-Gallegos, N., Carrera, E. M., Dehesa, J. S., Angulo, J. C., Antolín, J. and Soriano-Correa, C. (2009) 'Theoretic-information entropies analysis of nanostructures: ab initio study of PAMAM precursors and dendrimers G0 to G3', *Molecular Simulation*, 35:6, 498 — 511

**To link to this Article:** DOI: 10.1080/08927020902833087

**URL:** <http://dx.doi.org/10.1080/08927020902833087>

## PLEASE SCROLL DOWN FOR ARTICLE

Full terms and conditions of use: <http://www.informaworld.com/terms-and-conditions-of-access.pdf>

This article may be used for research, teaching and private study purposes. Any substantial or systematic reproduction, re-distribution, re-selling, loan or sub-licensing, systematic supply or distribution in any form to anyone is expressly forbidden.

The publisher does not give any warranty express or implied or make any representation that the contents will be complete or accurate or up to date. The accuracy of any instructions, formulae and drug doses should be independently verified with primary sources. The publisher shall not be liable for any loss, actions, claims, proceedings, demand or costs or damages whatsoever or howsoever caused arising directly or indirectly in connection with or arising out of the use of this material.

## Theoretic-information entropies analysis of nanostructures: *ab initio* study of PAMAM precursors and dendrimers G0 to G3

R.O. Esquivel<sup>abc\*</sup>, N. Flores-Gallegos<sup>c</sup>, E.M. Carrera<sup>c</sup>, J.S. Dehesa<sup>ab</sup>, J.C. Angulo<sup>ab</sup>, J. Antolín<sup>bd</sup> and C. Soriano-Correa<sup>c</sup>

<sup>a</sup>Departamento de Física Atómica, Molecular y Nuclear, Universidad de Granada, 18071 Granada, Spain; <sup>b</sup>Instituto Carlos I de Física Teórica y Computacional, Universidad de Granada, 18071 Granada, Spain; <sup>c</sup>Departamento de Química, Universidad Autónoma Metropolitana-Iztapalapa, San Rafael Atlixco No. 186, Col., Vicentina, C.P. 09340 México; <sup>d</sup>Departamento de Física Aplicada, EUITIZ, Universidad de Zaragoza, 50018 Zaragoza, Spain; <sup>e</sup>Laboratorio de Química Computacional, FES-Zaragoza, Universidad Nacional Autónoma de México, C.P. 09230 Iztapalapa, México

(Received 1 November 2008; final version received 16 February 2009)

Information theory in conjugated and in Hilbert spaces is employed to analyse the growing behaviour of nanostructures. Shannon entropies in position and momentum spaces require costly and time-consuming computations as the size of the molecules increases in contrast with information entropies in Hilbert space, which are shown to be highly advantageous for analysing large molecules. In this work, *ab initio* electronic structure calculations at the Hartree–Fock (HF), MP2 and B3LYP levels of theory were performed to analyse the initial steps towards growing nanostructured molecules of polyamidoamine (PAMAM) dendrimers, starting from the monomers, dimers, trimers and tetramers up to generations G0 (with 84 atoms), G1 (228 atoms), G2 (516 atoms) and G3 (1092 atoms). This was achieved by using selected physical descriptors such as the radius of gyration, the asphericity factor, the moments of inertia, the dipole moments, the total energies and chemical reactivity indices such as the hardness, softness and the electrophilicity index at the HF/3-21G\* level of theory. For the chemical indices, higher level calculations at the B3LYP/6-311++ G\*\* and MP2/6-311+ G\* levels were also performed in order to account for the effects of electron correlation. Information-theoretic measures of the Shannon type in conjugated space were employed to characterise the G0–PAMAM precursors and G0. Hilbert space entropies of the Shannon and Kullback type were employed to provide theoretic-information evidence of the validity of the dense-core model of PAMAM precursors and dendrimers G0 to G3.

**Keywords:** nanostructure; dendrimers; PAMAM; information theory; *ab initio* calculations

### 1. Introduction

Since their introduction in 1985 by Tomalia et al. [1], dendrimers have attracted much attention because of their fascinating structure and unique properties [2]. Dendrimers are globular, size monodisperse macromolecules in which all bonds emerge radially from a central focal point or core with a regular branching pattern and with units that repeat and contribute to a branch point. They are defined by three components: a central core; an internal dendritic structure (the branches); and an external surface with functional surface groups. Not all regularly branched molecules are dendrimers because of properties of the dendritic state [2b], such as core encapsulation [3]. These macromolecules were first synthesised in the early 1980s with the development of a cascade type of synthetic strategies to give distinct generations (G0, G1, G2, ...) of molecules with narrow molecular weight distribution, uniform size and shape and multiple (multivalent) surface groups [4]. Several applications for dendrimers have been proposed in the literature [5], with potential applications in

biology as mimetic systems of enzymes or redox proteins [6], in medicine for drug delivery, gene therapy and biochemical sensors [7], in optoelectronics for transduction of signals or light-harvesting devices [8] and in nanoscience as building units in self-assembled systems or functionalised with groups for molecular recognition and signalling [5a,b,9].

Polyamidoamine (PAMAM) dendrimers are among the most studied families of dendrimers. These organic dendrimers contain tertiary amines as branching points, i.e. the respective branching multiplicity is two. The core multiplicity varies; the original PAMAM dendrimers were synthesised from an amine core and thus had a threefold multiplicity [1,6a] whereas recently, ethylenediamine (EDA) core PAMAMs became more common and these possess a fourfold multiplicity, where the typical end groups are primary amines [10].

A number of review articles on dendrimers have been reported [5,8a,11]. Most of the reported work was motivated by a dendrimer model of a hollow core and

\*Corresponding author. Email: esqol@ugr.es

hence by a dense shell. The basic assumption behind this was that the density of the segments increases from the centre to the periphery, supporting the idea of using dendrimers as dendritic boxes or carriers. This dense-shell model became popular since the work of de Gennes and Hervet [12], in which they presented the first theoretical treatment of dendrimers by using a modified version of self-consistent field (SCF) method developed by Edwards [13], where they obtained a density profile with a global minimum at the centre and a monotonic density increasing towards the periphery of the dendrimer. Much of the work on synthesis of dendrimers and applications indicates that most studies are still based on this assumption. On the other hand, Lescanec and Muthukumar [14] performed the first simulations of dendrimers. They used a kinetic growth algorithm of self-avoiding walks to build off-lattice dendrimers and they found, in contrast with [12], density profiles that decreased monotonically towards the edge of the molecule. They were the first to show that a dendritic structure made up from flexible bonds should exhibit its maximum density at the centre of the molecule (dense-core model). This pioneering work has been the starting point of a considerable number of theoretical studies that support the early result of Lescanec and Muthukumar, thus firmly establishing the validity of the dense-core model.

Several theoretical approaches have been applied to the problem of the conformation of isolated dendrimers, the SCF method [12,15], the Gaussian variational approximation [16] and the Gaussian self-consistent theory [17]. Except for the work of de Gennes and Hervet [12], all of them support the dense-core model. Furthermore, a great deal of progress in the understanding of the conformations of dendrimers has been achieved through computer simulations at various levels of description, from the microscopic (atomistic) to the oversimplified ones with different methodologies: Monte Carlo (MC); molecular dynamics (MD); and Brownian dynamics [18]. Recently, Maiti et al. [19], performed a systematic series of fully atomistic MC–MD simulations on PAMAM–EDA-cored dendrimers from G0 to G11, to characterise the structure and properties of these molecules. They reported the Cartesian coordinates for a snapshot of the trajectory for each dendrimer from generation 3 to generation 11. On the electronic structure (ES) side, only a few Hartree–Fock (HF) and density functional theory (DFT) studies have addressed to study some structural, thermodynamic, electronic and vibrational aspects of low-order generation dendrimers (G0 and G1) [20]. To the best of our knowledge, there are no *ab initio* studies of the ES type, which address the problem of understanding the structural properties of PAMAM dendrimers of higher generations and the issue is not a simple one since these molecules possess an enormous number of energetically permissible

conformations and a large number of atoms (EDA–PAMAM dendrimers grow from 84 atoms for G0 up to 294,852 atoms for G11), which are beyond the present capabilities for the ES packages and present computers to attempt high-level *ab initio* calculations; notwithstanding, it remains a major goal of quantum chemistry to design strategies and methodologies, which could be applied to dendrimers of higher generations. These molecules have now become an important issue in the fields of polymer theory, the physics of soft matter and supramolecular chemistry.

A most challenging problem for chemistry and physics resides in characterising and measuring the interactions between the different parts of a quantum system, which are thought as those essential pieces of the whole system which may explain the chemical reactivity and how to construct the formalism of more complex systems through the interplay of its constituting parts. In quantum chemistry, the concept of atoms in molecules (AIM) has been the focus of great deal of attention [21], since it provides a natural framework to study chemical reactivity of complex molecules by means of the interactions between atoms or functional groups and between different molecules when small density changes are produced. The real-space partitioning of a molecule into subsystems is still a challenging problem in theoretical chemistry [21,22], not only because of the arbitrary chemical frontiers that separate subsystems but also because of the high computational cost that is involved in the calculations. Atomic orbital-based population analyses are very popular in chemistry and though they allow for the partition of the molecular wave function into atomic contributions, they are not rotationally invariant and may produce negative populations [23]. However, there exist alternative schemes that avoid these drawbacks, for instance, the natural atomic orbital scheme of Weinhold [24] or the one of Davidson–Löwdin [25]. For this purpose, Löwdin's [26] symmetric orthogonalisation on the atomic orbitals of the same atom has been considered as the most useful. In defining these schemes, one can preserve to a maximum extent the information content of ground state atoms to obey physical principles such as the N- and v-representabilities. Further, information-theoretic principles can be employed to define suitable natural probabilities for analysing interactions between molecular units or fragments in a molecule, which in turn allow for more involved chemical studies such as reactivity, conformational analysis, similarity, reactions, dissociation processes, etc. [27]. To the best of our knowledge, and notwithstanding that there has been a great interest in the last years in applying information theory (IT) measures to the ES of atoms and molecules in a wide variety of fields [28], no IT studies have been performed on nanostructures of the dendrimer type.

Through the present investigation, we will show that despite the limitations of quantum chemistry methods, it is possible to apply chemical concepts to elucidate some of the structural features of dendrimers. One of the goals is to support the validity of the core-dense model for dendrimers from a theoretic-information point of view. Besides, we will employ some selected polymer science properties of dendrimers to reveal the growing behaviour of PAMAM precursors and the G0 dendrimer at the HF level of theory along with several chemical reactivity parameters within the context of conceptual DFT. Higher level calculations at the DFT-B3LYP and MP2 levels of theory will be attempted to take into account the effects of electron correlation on the chemical indices. Finally, we will show that information entropies in Hilbert space are able to reveal the growing behaviour of PAMAM-EDA nanostructures up to G3 with significant computational advantages when compared with the calculation of standard Shannon entropies in position and momentum spaces.

## 2. Theoretical details

Throughout the study, we will employ several physical descriptors commonly used in polymer science and in theoretical chemistry which will be defined in this section. The principal moments of inertia  $I_x$ ,  $I_y$  and  $I_z$  are calculated through the eigenvalues of the shape tensor  $\mathbf{G}$  describing the mass distribution

$$\mathbf{G}_{pq} = \left( \frac{1}{M} \right) \left[ \sum_i^N m_i (r_{pi} - R_p)(r_{qi} - R_q) \right], \quad (1)$$

where  $p, q = x, y, z$ , and  $r_{pi}$  is the position of the  $i$ th atom relative to the  $R_p$  components of the centre of mass of the molecule;  $M$  is the mass of the molecule; and  $m_i$  is the mass of the atom. The sum of three eigenvalues ( $I_x$ ,  $I_y$  and  $I_z$ ) is an invariant of the shape tensor  $\mathbf{G}$ , giving  $\langle R_g^2 \rangle$ , which is the mean square radius of gyration that provides a quantitative characterisation of the dendrimer size. The ratio of these three principal moments is a measure of *eccentricity* (minor-major axes ratio) of the shape ellipsoid of the dendrimers, and hence the shape of the dendrimer can be assessed from the values of the ratio of the three principal moments of inertia of the molecules  $I_z/I_y$  and  $I_z/I_x$ . Rudnick and Gaspari [29] introduced a better definition of *asphericity* frequently used in the literature as

$$\delta = 1 - 3 \frac{\langle I_2 \rangle}{\langle I_1^2 \rangle}, \quad (2)$$

where  $I_i$  are the respective invariants of the gyration tensor and are given by

$$I_1 = I_x + I_y + I_z \quad (3)$$

and

$$I_2 = I_x I_y + I_x I_z + I_y I_z. \quad (4)$$

We have also evaluated some reactivity parameters that may be useful to analyse the chemical properties of the precursors. Parr and Pearson [30] proposed a quantitative definition of hardness ( $\eta$ ) within conceptual DFT

$$\eta = \frac{1}{2S} = \frac{1}{2} \left( \frac{\partial \mu}{\partial N} \right)_{\nu(r)} \quad \text{where } \mu = \left( \frac{\partial E}{\partial N} \right)_{\nu(r)}, \quad (5)$$

is the electronic chemical potential of an  $N$  electron system in the presence of an external potential  $\nu(r)$ ;  $E$  is the total energy; and, in the context of DFT, ‘ $S$ ’ is called the softness. Using finite difference approximation, Equation (9) would be

$$\eta = \frac{1}{2S} \approx \frac{E_{N+1} - 2E_N + E_{N-1}}{2} = \frac{I - A}{2}, \quad (6)$$

where  $E_N$ ,  $E_{N-1}$  and  $E_{N+1}$  are the energies of the neutral, cationic and anionic systems, and  $I$  and  $A$  are the ionisation potential and electron affinity, respectively. Applying Koopmans’ theorem [31] Equation (6) can be written as

$$\eta = \frac{1}{2S} \approx \frac{\varepsilon_{\text{LUMO}} - \varepsilon_{\text{HOMO}}}{2}, \quad (7)$$

where  $\varepsilon$  denotes the frontier molecular orbital energies. In general terms, hardness and softness are good descriptors of chemical reactivity, the former measures the global stability of the molecule (larger values of  $\eta$  means less reactive molecules), whereas the ‘ $S$ ’ index quantifies the polarisability of the molecule [32], thus soft molecules are more polarisable and possess predisposition to acquire additional electronic charge [33]. The chemical hardness ‘ $\eta$ ’ is a central quantity for use in the study of reactivity and stability, through the hard and soft acids and bases principle [34].

On the other hand, Parr et al. [35] have defined another descriptor in order to quantify the global electrophilic power of the molecules, namely the electrophilicity index  $\omega$ , which defines a quantitative classification of the global electrophilic nature of a molecule within a relative scale. Electrophilicity index of a system in terms of its chemical potential and hardness is given by the next expression

$$\omega = \frac{\mu^2}{2\eta}. \quad (8)$$

In general terms, hardness and electrophilicity are good descriptors of chemical reactivity, the former measures the global stability of the molecule (larger values of  $\eta$  means less reactive molecules), whereas the  $\omega$  index quantifies the global electrophilic power of the

molecules (predisposition to acquire an additional electronic charge) [33].

According to the goals of the present study, the central quantities in real space are the Shannon [36] entropies, either in position or momentum spaces

$$S_r = - \int \rho(r) \ln \rho(r) d^3r, \quad (9)$$

$$S_p = - \int \gamma(p) \ln \gamma(p) d^3p, \quad (10)$$

where  $\rho(r)$  and  $\gamma(p)$  are normalised to unity and denote the molecular electron density distributions in the position and momentum spaces, respectively. The Shannon entropy behaves like a measure of delocalisation or lack of structure of the electronic density in the position space, and hence  $S_r$  is maximal when knowledge of  $\rho(r)$  is minimal. The Shannon entropy in momentum space  $S_p$  is the largest for systems with electrons of higher speed and is smaller for relaxed systems, where kinetic energy is low. Entropy in momentum space  $S_p$  is closely related to  $S_r$  by the uncertainty relation of Bialynicki-Birula and Mycielski [37], which shows that the entropy sum  $S_T = S_r + S_p$ , is a balanced measure and cannot decrease arbitrarily. For one-electron atomic systems, it may be interpreted as that localisation of the electron's position results in an increase in the kinetic energy and a delocalisation of the momentum density.

From a different perspective, we have recently shown [27] that there is an information-theoretic justification for performing Lowdin [38] symmetric transformations on the atomic Hilbert space, to produce orthonormal atomic orbitals of maximal occupancy for the given wave function, which are derived in turn from atomic angular symmetry subblocks of the density matrix, localised on a particular atom and transforming to the angular symmetry of the atoms. The advantages of these kind of AIM approaches [39,40] are that the resulting natural atomic orbitals are N-representable, positively bounded and rotationally invariant [25,41]. In consequence, we have also shown [42] that the corresponding 'natural atomic probabilities' (NAP) are useful to define von Neumann information entropies in Hilbert space, which are able to measure entanglement in the context of quantum IT [43].

The uncertainty of a probability distribution  $p_i(A)$  is measured through the Shannon [44] entropy in Hilbert space

$$H(A) = - \sum_i p_i(A) \ln p_i(A). \quad (11)$$

The relative entropy between two probability distributions  $p_i(A)$  and  $p_i(B)$  is defined through the

Kullback–Liebler entropy [45] as

$$H(A||B) = \sum_i p_i(A) \ln \frac{p_i(A)}{p_i(B)}, \quad (12)$$

where the  $p_i(A)$  (and  $p_i(B)$ ) in Equations (11) and (12) can be determined by the use of NAP [27,42]. It is worth noting that while Equation (12) represents a distance from a reference probability, it fails to be symmetric.

### 3. Results and discussion

The ES calculations performed in this study were carried out with the NwChem suite of programs [46] at the HF/3-21G\* and B3LYP/6-311++G\*\* levels of theory and with the Gaussian/G03 suite of programs [47] for calculations at the MP2/6-311+G\* level of theory. The systems under analysis are precursors of PAMAM–EDA G0, i.e. EDA ( $C_2H_4(NH_2)_2$ ), the PAMAM monomer ( $NH_2-CH_2-CH_2-CO-NH-CH_2-CH_2-NH_2$ ), the dimer (EDA+monomer), the trimer (EDA+2 monomers) and the tetramer (EDA+3 monomers) along with some of the conformers of these systems, which were optimised at the levels of theory required for each property as mentioned below. The G0 geometry for the IT study in real space along with the geometries G1–G3 employed for the IT study in Hilbert space were obtained from Maiti<sup>1</sup> [19] and then calculated at the HF/3-21G\* level [46]. In order to determine the information entropies in Hilbert space,  $H(A)$  and  $H(A|B)$ , we employed NAP [27] calculated with the NBO 5.G software [48]. The molecular Shannon information entropies in position and momentum spaces were obtained by employing software developed in our laboratory along with the three-dimensional numerical integration routines by Pérez-Jordá et al. [49] and the DGRID suite of programs by Kohout [50]. Besides, several ES properties were calculated in order to analyse the shape of the polymers, the aspect ratios, the asphericity factor and the dipole moment components, along with several DFT chemical reactivity properties such as the frontier orbital energies (HOMO and LUMO), hardness, softness and the electrophilicity values. Since these chemical properties might be sensitive to the electron correlation and basis set quality, we have performed calculations at the MP2/6-311+G\* and B3LYP/6-311++G\*\* levels of theory. Optimised structures at each level were determined in order to obtain reliable values for chemical reactivity parameters.

In Table 1, we have reported the total dipole moment values for all polymeric structures from EDA to G0 along with the dipole moment components, which are also shown in Figure 1 from which we can witness an increase in the polarisation of the molecular densities in all directions as the molecules grow, with larger effects for G0. This might be indicative of more polarisable densities,

Table 1. Values for the total dipole moment and its components (Debye) for the PAMAM-G0 precursors and G0 dendrimer calculated at the HF/3-21G\* level of theory.

Molecule	$\mu_x$	$\mu_y$	$\mu_z$	$\mu_{TOTAL}$
EDA	0.0	0.0	0.0	0.0
M1	-0.477	0.745	0.699	3.365
M2	1.073	0.702	0.594	2.509
M3	1.073	0.702	0.594	5.826
M4	0.042	0.916	0.481	2.368
M5	-0.216	0.644	0.969	2.583
D1	-0.814	-1.678	4.490	4.479
D2	1.131	-3.314	-0.221	4.334
T1	0.164	0.893	1.389	2.267
TT1	3.114	-0.450	-1.227	3.377
TT2	4.729	1.060	1.075	4.964
G0	3.041	-7.293	1.488	3.241

which in turn may reflect molecular densities that tend to be more delocalised.

It is known that flexible-chain dendrimers, although being chemically regular structures, do not assume regular shapes. To quantitatively evaluate the deviation from spherical symmetry, we calculated the shape of the precursors and G0 dendrimer through several physical quantities: the principal moments of inertia  $I_x$ ,  $I_y$  and  $I_z$  (Equation (1)); the ratio of the three principal moments of inertia of the molecules  $I_z/I_y$  and  $I_z/I_x$ ; the asphericity factor (Equation (2)); and the dendrimer size (measured through the radius of gyration, which is the mean square of

the sum of the moments of inertia). The values of the three principal moments of inertia are tabulated in Table 2, along with the radius of gyration and the asphericity factor, while Figures 2–4 show the moment of inertia ratios, the radius of gyration and the asphericity factor, respectively, for the different G0 precursors and the G0 dendrimer.

From Table 2 and Figure 2, we may assess the size of the dendrimers through the radius of gyration. As expected,  $R_g$  values show a constant increasing trend in going from the monomers up to the G0 dendrimer. The shape of the G0 precursors and G0 dendrimer can be assessed from the values of the ratio of the three principal moments of inertia of the molecules  $I_z/I_y$  and  $I_z/I_x$  in Figure 3 from which we observe that all the precursors are more eccentric than the G0 generation, which tend to be more spherical. A quantity that reflects this fact in a more precise manner is the asphericity factor, which is depicted in Figure 4, where it may be observed that dendrimer G0 tend to be more spherical when compared with the rest of the G0 precursors, except for the M4 monomer whose conformeric structure is not linear.

On the chemical side, we have also evaluated some reactivity parameters that may be of utility to analyse the chemical properties of the precursors. In general terms, hardness and electrophilicity are good descriptors of chemical reactivity, the former measures the global stability of the molecule (larger values of  $\eta$  means less reactive molecules), whereas the  $\omega$  index quantifies the global electrophilic power of the molecules (predisposition to

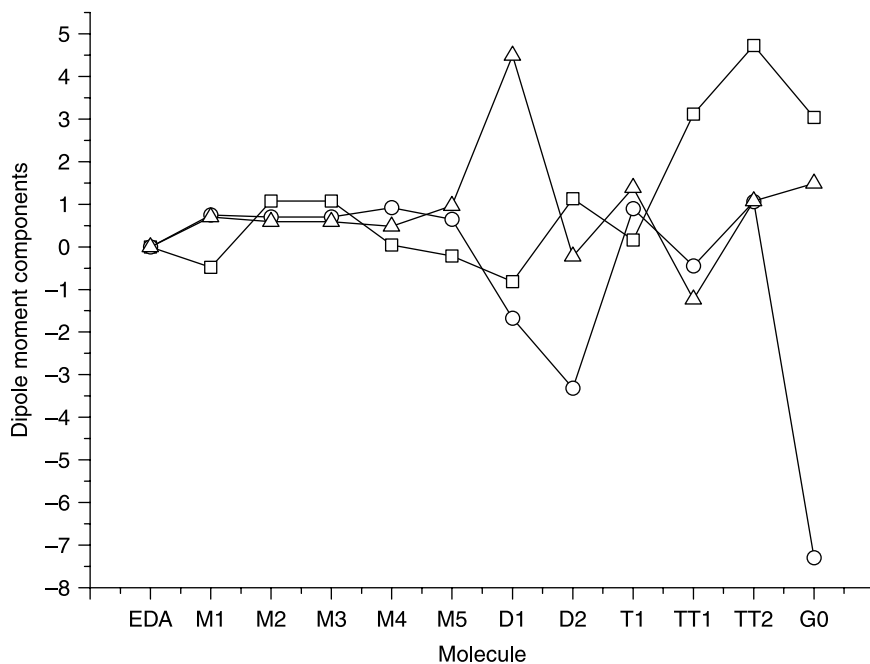


Figure 1. Dipole moment components in Debyes for the PAMAM polymeric precursors and the G0 dendrimer structure at the HF/3-21G\* level. (unfilled squares,  $\mu_x$ ; unfilled circles,  $\mu_y$ ; and unfilled triangles,  $\mu_z$ ).

Table 2. Values for the principal moments of inertia  $I_x$ ,  $I_y$ ,  $I_z$  (a.u.), the radius of gyration ( $R_g$ ; a.u.) and the parameter of asphericity  $\delta$  for the precursors and dendrimer G0 calculated at the HF/3-21G\* level of theory.

Molecule	$I_x$	$I_y$	$I_z$	$R_g$	$\delta$
EDA	486	71	495	32.4	0.159
M1	3001	1044	2823	82.8	0.075
M2	2089	3218	1571	82.9	0.045
M3	2090	3218	1571	82.9	0.045
M4	1762	1574	1813	71.8	0.002
M5	1721	3028	1965	81.9	0.032
D1	3152	5286	6231	121.1	0.035
D2	5174	2142	6782	118.7	0.084
T1	14,936	18,993	32,820	258.4	0.059
TT1	21,767	26,043	42,123	300.0	0.043
TT2	28,212	20,641	43,350	303.6	0.047
G0	42,929	46,745	26,720	341.2	0.025

acquire an additional electronic charge) [33]. In Table 3, we have reported values for the total energies, the frontier orbital energies HOMO and LUMO, the hardness and the electrophilicity index. These values were calculated at three different levels of theory: HF/3-21G\*; B3LYP/6-311++G\*\*; and MP2/6-311+G\*, in order to take into account with the effects of electron correlation. It is worth mentioning that geometry optimisation for each precursor was performed at every level of theory. The different values are reported in Table 3 for comparison purposes. Also we have depicted the values for the hardness and the electrophilicity index in Figures 5 and 6, respectively,

at the HF, B3LYP and MP2 levels of theory as to analyse the general trends and also the effects for electron correlation.

From Table 3 and Figures 5 and 6, we may note that hardness values show a clear decreasing tendency as the molecules are bigger in size for the three levels of theory, which means that as the size of the precursor increases toward G0 the polarisability of the molecules increases, i.e. their corresponding densities tend to be more delocalised and hence more reactive in chemical terms with the G0 dendrimer being the most reactive. It is also interesting to note that hardness values are smaller as correlation increases, which is in agreement with the energy trends observed from Table 3, in that the B3LYP energy values are negatively larger than MP2 ones and these are in turn more negative than the HF values. On the other hand, the electrophilicity behaviour may be analysed from Figure 6, which roughly indicates a tendency to acquire electronic charge, i.e. as the size of the precursors increase they are more polarisable and hence more reactive, except for the tetramer precursors (TT1 and TT2) that show smaller values for correlated methods when compared with the rest. It is also worth mentioning that as correlation increases from HF values to B3LYP ones, the electrophilicity values increase, which agrees with Equation (8) in that electrophilicity is inversely proportional to the hardness, and this is what we observed from Figures 5 and 6.

Observations above are in agreement with the results for the dipole moment components, in that higher generation dendrimers possess more polarised molecular

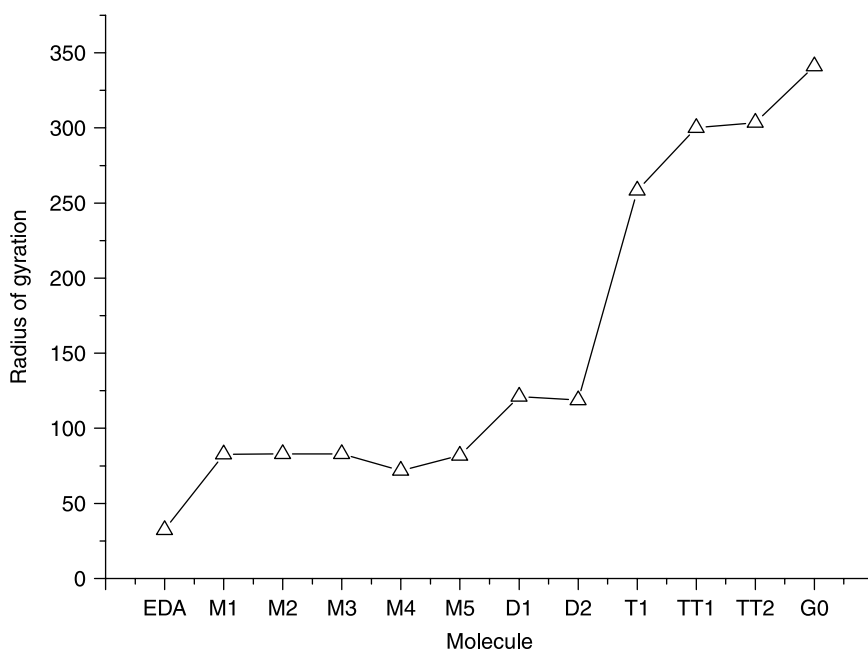


Figure 2. The radius of gyration  $R_g$  as a function of generation for the G0 precursors and the G0-PAMAM dendrimer calculated at the HF/3-21G\* level of theory.

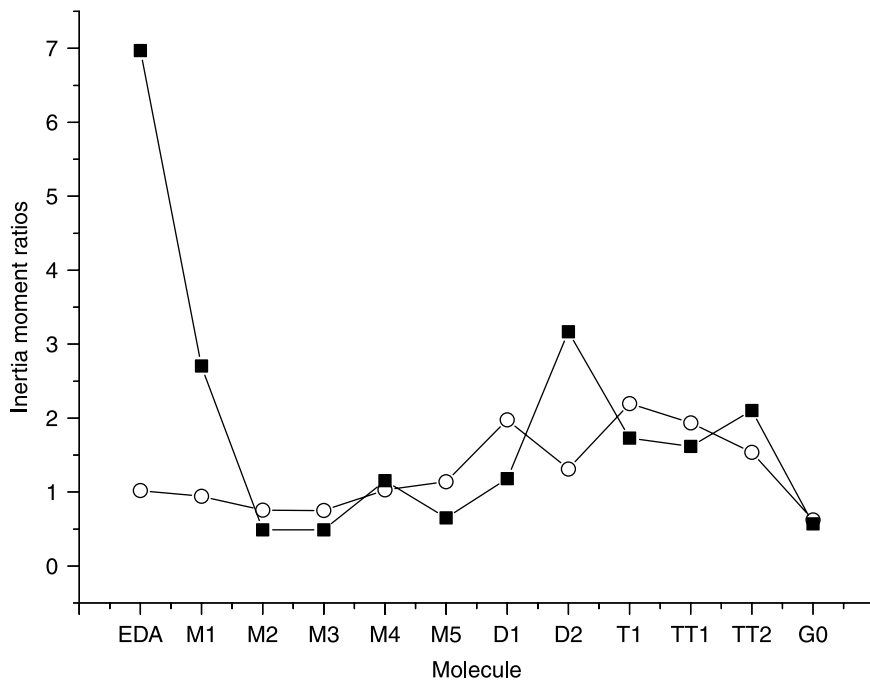


Figure 3. Moment of inertia aspect ratios  $I_z/I_x$  (unfilled circles),  $I_z/I_y$  (filled squares) for the G0 precursors and the G0-PAMAM dendrimer calculated at the HF/3-21G\* level of theory.

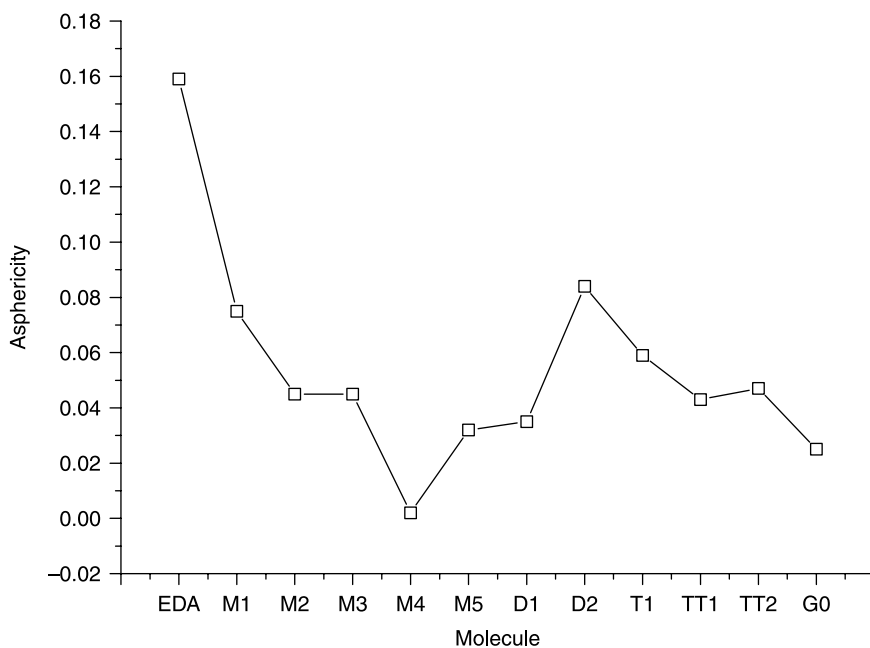


Figure 4. The asphericity parameter  $\delta$  as a function of generation for the G0 precursors and the G0-PAMAM dendrimer calculated at the HF/3-21G\* level of theory.



Table 3. Values for the total energies, frontier orbital energies, hardness ( $\eta$ ) and the electrophilicity index ( $\omega$ ) in atomic units for the G0 precursors and dendrimer G0 at the HF/3-21G\* (first row), MP2/6-311+G\* (second row) and B3LYP/6-311++ G\*\* (third row) levels.

Molecule	Energy	$\epsilon_{\text{HOMO}}$	$\epsilon_{\text{LUMO}}$	$\eta$	$\omega$
EDA	-188.210	-0.351	0.267	0.309	0.0028
	-189.941	-0.372	0.072	0.222	0.050
	-190.582	-0.232	-0.011	0.111	0.067
M1	-432.691	-0.352	0.210	0.281	0.0090
	-436.621	-0.385	0.059	0.222	0.060
	-437.982	-0.244	-0.023	0.111	0.080
M2	-432.697	-0.355	0.211	0.283	0.0092
	-436.627	-0.375	0.056	0.215	0.059
	-437.987	-0.247	-0.019	0.114	0.077
M3	-432.697	-0.355	0.211	0.283	0.0092
	-436.628	-0.375	0.056	0.215	0.059
	-437.986	-0.231	-0.025	0.103	0.080
M4	-432.700	-0.354	0.207	0.281	0.0097
	-436.631	-0.381	0.065	0.223	0.056
	-437.989	-0.236	-0.017	0.110	0.073
M5	-432.701	-0.356	0.221	0.288	0.0079
	-436.631	-0.378	0.063	0.221	0.056
	-437.990	-0.239	-0.021	0.109	0.077
D1	-565.030	-0.336	0.210	0.273	0.0073
	-570.184	-0.365	0.058	0.211	0.056
	571.987	-0.225	-0.021	0.102	0.074
D2	-565.035	-0.338	0.203	0.271	0.0085
	-570.191	-0.369	0.061	0.215	0.055
	-571.992	-0.227	-0.019	0.104	0.072
T1	-941.852	-0.329	0.206	0.268	0.0070
	-950.434	-0.354	0.050	0.202	0.057
	-953.390	-0.214	-0.026	0.094	0.077
TT1	-1318.630	-0.328	0.185	0.256	0.0099
	-1330.680	-0.343	0.056	0.199	0.052
	-1334.798	-0.209	-0.024	0.092	0.073
TT2	-1318.639	-0.327	0.187	0.257	0.0095
	-1330.690	-0.341	0.059	0.200	0.050
	-1334.806	-0.207	-0.023	0.092	0.072
G0	-1695.442	-0.315	0.172	0.244	0.0105
	-1710.928	-0.334	0.039	0.186	0.058
	-1716.198	-0.203	-0.032	0.086	0.080

densities. Further, it is known that less compact molecules are more polarisable, with low hardness values and hence more reactive, and this is indeed the case when comparing the softness values depicted in Figure 7 with the size of the molecules, which can be estimated through the radius of gyration  $R_g$  shown in Figure 2.

Next, we examine the Shannon information entropies in real space, Equations (9) and (10). In Figure 8, the entropy sum,  $S_r + S_p$ , and the energy (Table 3) are depicted for the PAMAM G0 precursors and dendrimer G0. It is apparent from Figure 8 that the total entropy follows the opposite behaviour as the energy, i.e. as the size of the molecules increases so does the entropy sum. It is also interesting to note that the total entropy

distinguishes the different polymeric structures, in that isoelectronic systems possess the same entropy value and so does the energy.

Moreover, a similar behaviour is shown in Figure 9, where the Shannon entropies in position and momentum spaces are depicted at the HF/3-21G\* level. Whereas the momentum space entropies are fairly constant for all systems, the position entropy reveals more structure, in that as the size of the precursor increases there is a clear trend to get more delocalised densities and hence less compact structures, which tend to be more polarisable as discussed above (Figure 7). This observation is in fair agreement with the dense core model as a growing model for dendrimers. In contrast, the momentum space entropy does not show significant changes among the different structures, as the dispersion of the values for this measure is very small when compared with the position entropy.

Finally, we investigate the information entropies in Hilbert space, Equations (11) and (12), in connection with the growing behaviour of PAMAM dendrimers. It is important to mention that whereas Shannon entropies in real space represent costly and time consuming calculations, Hilbert space entropies do not pose additional computational efforts as to the theoretic-information analyses concerns; of course, the obtaining of the wave functions and the NAP values represents a challenge for ES calculations and the present computation capabilities available to us. Thus, we have performed the necessary calculations at the HF/3-21G\* level for analysing additional structures, the trimer conformations T2, T4 and T6, along with G1–G3 dendrimers (G1 with 228 atoms, G2 with 516 atoms and G3 with 1092 atoms). In Figure 10, we have depicted the Shannon entropy  $H(A)$  for all the PAMAM G0 precursors along with the G0–G3 dendrimers. This measure allows to determine the global information content of the systems, and consequently we may observe from Figure 10 that  $H(A)$  shows an increasing behaviour as the size of the precursors and dendrimers increases. This again supports the above discussed dense-core model of dendrimers as bigger molecules show more uncertainty in Hilbert space, which corresponds to less compact densities in real space and hence to more delocalised electronic distributions.

Furthermore, in Figure 11, we have plotted the Kullback–Leibler relative entropy in Hilbert space  $H(A|B)$ , along with the total energy values for all dendrimer precursors and dendrimers G0–G3, calculated at the HF/3-21G\* level. The Kullback–Leibler measure represents a distance from a reference probability distribution, which in this case we have set for the EDA molecule (which is embedded in all the structures). We may observe from the Figure 11 that as the molecules depart from EDA, the Hilbert information distance increases in a monotonically fashion that reflects the

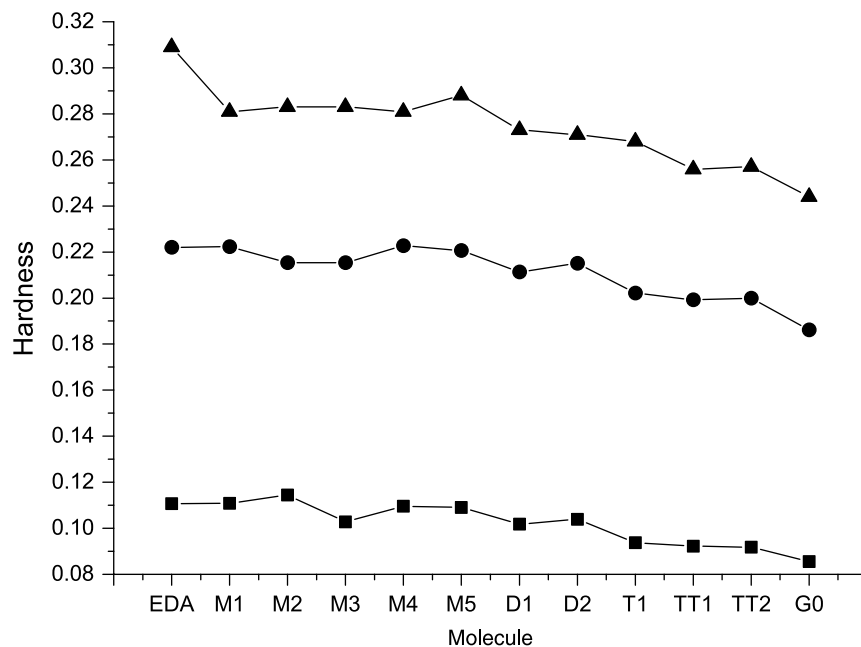


Figure 5. The hardness  $\eta$  values for the G0 precursors and G0 dendrimer at the HF/3-21G\* (filled triangles), the MP2/6-311+G\* (filled circles) and at the B3LYP/6-311++ G\*\* (filled squares) levels of theory.

core-dense growing behaviour of dendrimers by simply measuring the information distance between EDA and the increasingly bigger molecules. Assuming that dendrimers follow a hollow-core model of growth and hence a dense-shell model, the  $H(A|B)$  trend would have been just the opposite.

Interestingly, Figures 10 and 11 show the ability of these quantum measures to reveal and corroborate two simple facts already discussed in the literature [51]<sup>2</sup>: (1) the validity of the core-dense model witnessed by the mutual von Neumann entropy of the marginal type, as the  $H(A|B)$  Hilbert distance increases monotonically in

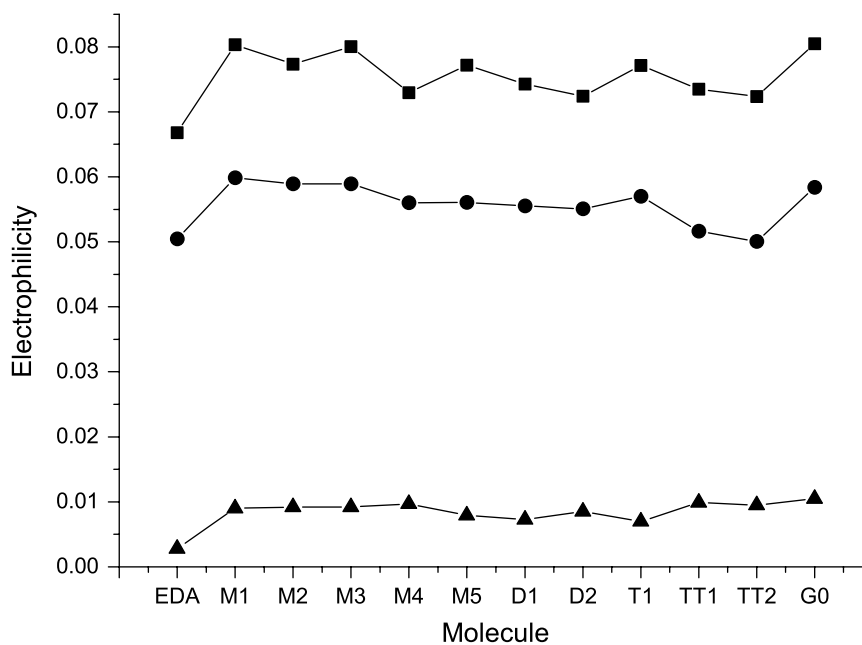


Figure 6. The electrophilicity index for the G0 precursors and the G0 dendrimer at the HF/3-21G\* (filled triangles), the MP2/6-311+G2mu\* (filled circles) and at the B3LYP/6-311++ G\*\* (filled squares) levels of theory.

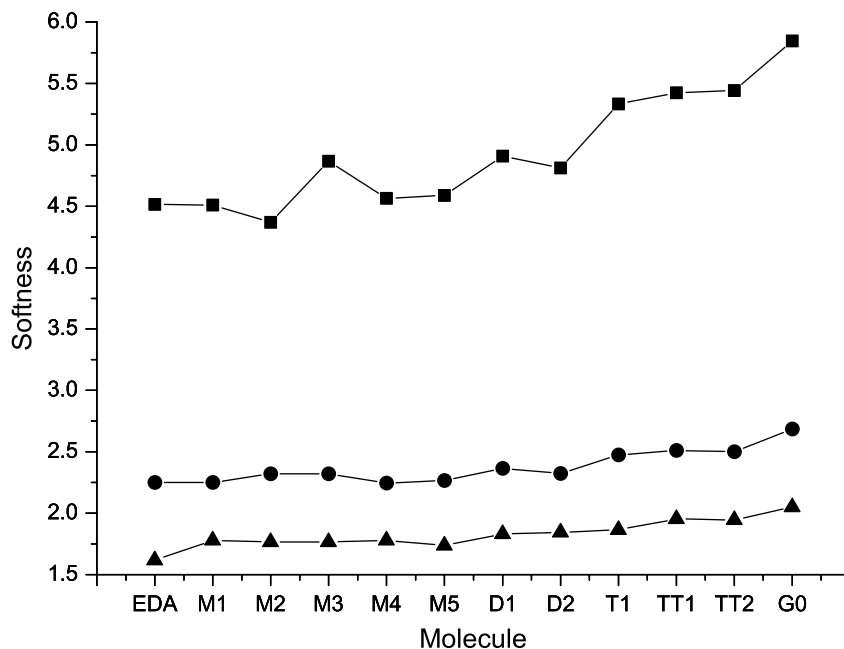


Figure 7. The softness 'S' values for the G0 precursors and the G0 dendrimer at the HF/3-21G\* (filled triangles), the MP2/6-311+G\* (filled circles) and at the B3LYP/6-311++ G\*\* (filled squares) levels of theory.

going from the precursors to higher generation dendrimers; and (2) the global information content of the systems,  $H(A)$ , which increases monotonically as one would expect from a thermodynamic point of view

(entropy). A particular feature that may be noted from Figure 9 is the capacity of  $H(A)$  of measuring the atomic and electronic contents of the systems, regardless of its conformational structure, which is characteristic of

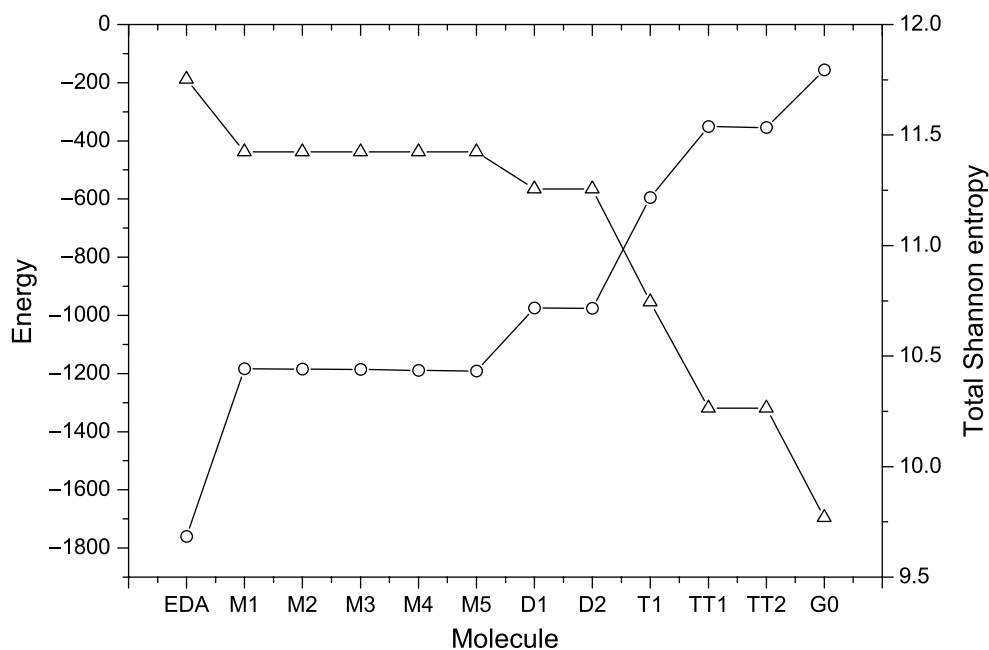


Figure 8. Shannon entropy sum (unfilled circles) and the total energies in a.u. (unfilled triangles) for the PAMAM polymeric precursors at the HF/3-21G\* level.

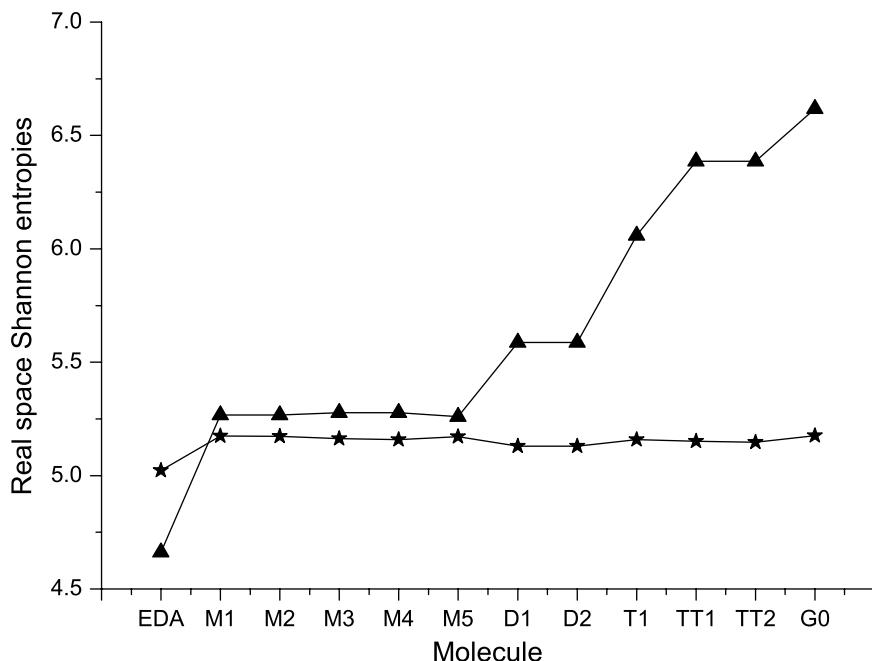


Figure 9. Shannon entropies in position (filled triangles) and momentum (stars) spaces (Equations (9) and (10)) for the G0 precursors and the G0 dendrimer at the HF/3-21G\* level.

the energy. The relevancy of these results might be assessed by considering that the equivalent information in real space implied the calculation of position and momentum space entropies of the Shannon type which, taking into account the size of the systems (1023 atoms for G3 dendrimer), represents indeed a formidable task

to compute, even by taking into consideration that the integration quadratures were guided by promolecular grids. Ongoing research is being undertaken in our laboratories to extend the study to higher generation PAMAM dendrimers mainly on the side of the Hilbert space framework.

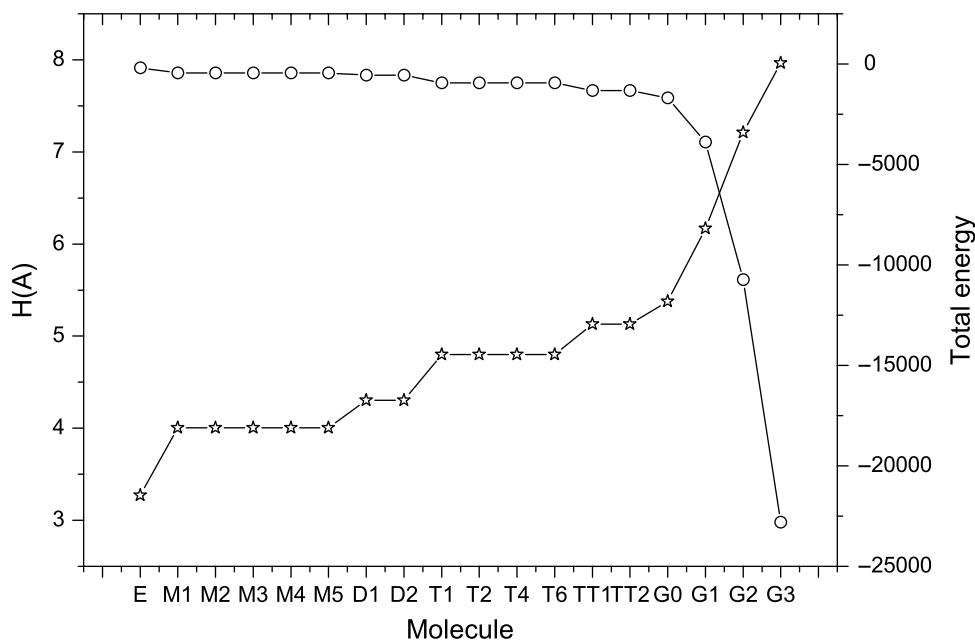


Figure 10. Shannon entropy in Hilbert space,  $H(A)$  from Equation (9) (stars), and the total energy values at the HF/3-21G\* level in a.u. (unfilled circles) for the G0 precursors and generations G0–G3. E stands for the EDA molecule.

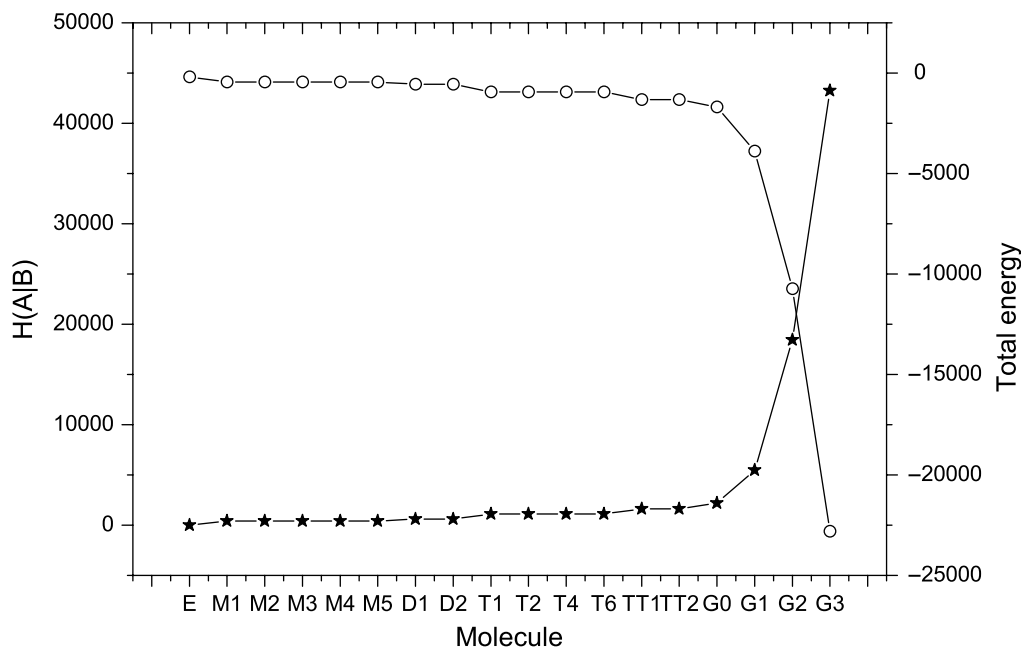


Figure 11. Kullback–Leibler entropy in Hilbert space,  $H(A|B)$  from Equation (10) (stars), and the total energy values in a.u. at the HF/3-21G\* level (filled circles) for the G0 precursors and generations G0–G3. E stands for the EDA molecule.

#### 4. Conclusion

Throughout this investigation, we have employed selected polymer science parameters along with chemical reactivity descriptors, which show numerical evidence supporting the dense-core model of dendrimers. Besides, we have corroborated through higher level calculations, which take into account the effects of electron correlation, that the behaviour observed at the HF level depicts basically the same physical and chemical features. These results allow us to perform a more demanding computational study at the HF level in order to study the growing behaviour of dendrimer precursors from a theoretic-information perspective. Thus, it was shown that Shannon entropies defined in real space,  $S_r$  and  $S_p$ , as well as the information measures in Hilbert space,  $H(A)$  and  $H(A|B)$ , are capable of revealing the dense-core growing behaviour of dendrimers, by showing that bigger molecules possess more delocalised electronic distributions in such a way to span their molecular distributions as the molecular size increases.

To the best of our knowledge, the results presented in this work represent benchmark calculations for ES *ab initio* studies at three different levels of theory and with the inclusion of electron correlation. Thus, from the present study, we may conclude that it is feasible to employ ES *ab initio* methods to analyse PAMAM–EDA dendrimers, at least for low levels of theory, revealing the same basic features of more thorough studies of MC and atomistic MD type [19]. It is also worth mentioning that chemical reactivity indices like the ones employed here

may provide deeper insights into the structural properties and growing behaviour of dendrimers. An important result of this work is the application of Hilbert space information measures to PAMAM dendrimers, which were shown to reveal the same basic features of equivalent information measures in real space, which require much more expensive computations.

#### Acknowledgements

We wish to thank José María Pérez-Jordá and Miroslav Kohout for kindly providing with their numerical codes. R.O.E. wishes to thank Juan Carlos Angulo and Jesús Sánchez-Dehesa for their kind hospitality during his sabbatical stay on the Departamento de Física Atómica, Molecular y Nuclear at the Universidad de Granada, Spain. We acknowledge financial support through Mexican grants 82266 CONACYT, PIFI 3.3 PROMEP–SEP and Spanish grants MICINN projects FIS-2008-02380, FIS-2005-06237 (J.A.), FQM-1735, P05-FQM-00481 and P06-FQM-2445 of Junta de Andalucía. J.C. A. and J.A. belong to the Andalusian research group FQM-0207. E.M.C. wishes to thank CONACYT (México) for a PhD fellowship. Allocation of supercomputing time from the Departamento de Supercomputo at DGSCA–UNAM, the Sección de Supercomputacion at CSIRC–Universidad de Granada and the Laboratorio de Supercomputo y Visualización at UAM is gratefully acknowledged.

#### Notes

1. The geometric parameters of dendrimers G0–G3 were obtained from Maiti (see [19]).
2. The grids obtained by use of AUTOM [49] were obtained by using promolecular densities as generating kernel functions.

For dendrimers G0–G3, with a relative tolerance of  $1 \times 10^{-5}$ , the grid consists of 4.3 million points (M), 10.6, 34, and 79.5 M, respectively. Roughly, each point takes 1 s in a high performance supercomputer (per processor). So that, it is highly desirable to employ large array supercomputers to accomplish this kind of studies in a reasonable time.

## References

- [1] D.A. Tomalia, H. Baker, J. Dewald, M. Hall, G. Kallos, S. Martin, J. Roeck, J. Ryder, and P. Smith, *A new class of polymers: starburst dendritic macromolecules*, *Polym. J.* 17 (1985), pp. 117–132.
- [2] (a) G.R. Newkome, C.N. Moorefield, and F. Vögtle, *Dendritic Molecules: Concepts, Synthesis, Perspectives*, Wiley-VCH, Weinheim, 1996; (b) J.M.J. Fréchet and D.A. Tomalia (eds.), *Dendrimers and Other Dendritic Polymers*, Wiley, Chichester, 2001.
- [3] S. Hecht and J.M. Fréchet, *Dendritic encapsulation of function: applying nature's site isolation principle from biomimetics to materials science*, *J. Angew. Chem. Int. Ed. Engl.* 40 (2001), pp. 74–91.
- [4] H.M. Janssen and E.W. Meijer, *Synthesis of Polymers: Materials Science and Technology Series*, A.D. Schüter, R.W. Cahn, P. Haasen, E.J. Kramer, eds., Wiley-VCH, Weinheim, 1999, pp. 403–458.
- [5] (a) M. Fischer and F. Vögtle, *Dendrimers: from design to application – a progress report*, *Angew. Chem. Int. Ed.* 38 (1999), pp. 884–905; (b) F. Zeng and S.C. Zimmerman, *Dendrimers in supramolecular chemistry: from molecular recognition to self-assembly*, *Chem. Rev.* 97 (1997), pp. 1681–1712; (c) O.A. Matthews, A.N. Shipway, and J.F. Stoddart, *Dendrimers: branching out from curiosities into new technologies*, *Prog. Polym. Sci.* 23 (1998), pp. 1–56; (d) P. Holister, C. Roman-Vas, and T. Harper, *Dendrimers*, Technology White Papers, Vol. 6, 2003, pp. 1–15.
- [6] (a) D.A. Tomalia, A.M. Naylor, and W.A. Goddard III, *Starburst dendrimers: Molecular-level control of size, shape, surface chemistry, topology, and flexibility from atoms to macroscopic matter*, *Angew. Chem. Int. Ed. Engl.* 29 (1990), pp. 138–175; (b) D.A. Tomalia, B. Huang, D.R. Swanson, H.M. Brothers II, and J.W. Klimash, *Structure control within poly(amidoamine) dendrimers: size, shape and regio-chemical mimicry of globular proteins*, *Tetrahedron* 59 (2003), pp. 3799–3813; (c) H.-F. Chow, T.K.-K. Mong, Y.-H. Chan, and C.H. Cheng, *A new class of protein mimics: preparation and electrophoretic properties of polycationic  $\beta$ -alanine-based properties*, *Tetrahedron* 59 (2003), pp. 3815–3820; (d) F. Diederich and B. Felber, *Supramolecular chemistry and self-assembly special feature: supramolecular chemistry of dendrimers with functional cores*, *Proc. Natl. Acad. Sci. USA* 99 (2002), pp. 4778–4785; (e) L. Liu and R. Breslow, *Dendrimeric pyridoxamine enzyme mimics*, *J. Am. Chem. Soc.* 125 (2003), pp. 12110–12111.
- [7] F. Zeng and S.C. Zimmerman, *Dendrimers in supramolecular chemistry: from molecular recognition to self assembly*, *Chem. Rev.* 97 (1997), pp. 1681–1712.
- [8] (a) F. Vögtle, S. Gestermann, R. Hesse, H. Schwierz, and B. Windisch, *Functional dendrimers*, *Prog. Polym. Sci.* 25 (2000), pp. 987–1041; (b) A. Adronov and J.M. Fréchet, *Light harvesting dendrimers*, *J. Chem. Commun.* 18 (2000), pp. 1701–1710; (c) A.W. Freeman, S.C. Koene, P.R.L. Malenfant, M.E. Thompson, and J.M.J. Fréchet, *Dendrimer-Containing Light-Emitting Diodes: Toward Site-Isolation of Chromophores*, *J. Am. Chem. Soc.* 122 (2000), pp. 12385–12386; (d) V. Balzani, P. Ceroni, S. Gestermann, C. Kauffmann, M. Gorkab, and F. Vögtle, *Dendrimers as fluorescent sensors with signal amplification*, *Chem. Commun.* 10 (2000), pp. 853–854.
- [9] (a) J.M. Fréchet, *Dendrimers and supramolecular chemistry*, *J. Proc. Natl. Acad. Sci. USA* 99 (2002), pp. 4782–4787; (b) S.C. Zimmerman and V. Zeng, *Self-assembling dendrimers*, *Science* 271 (1996), pp. 1095–1098; (c) J.F.G.A. Jansen and E.W. de Brabander, *Encapsulation of guest molecules into a dendritic box*, *Science* 266 (1994), pp. 1226–1229.
- [10] S. Jockush, J. Ramirez, K. Sanghvi, R. Nociti, N.J. Turro, and D.A. Tomalia, *Comparison of nitrogen core and ethylenediamine core starburst dendrimers through photochemical and spectroscopic probes*, *Macromolecules* 32 (1999), pp. 4419–4423.
- [11] (a) M. Ballauff, *Dendrimers III: design, dimension, function*, *Top. Curr. Chem.* 212 (2001), pp. 177–194; (b) D. Pötschke and M. Ballauff, *Structure of dendrimers in solution as probed by scattering experiments*, in *Structure and Dynamics of Polymer and Colloidal Systems*, R. Borsali and R. Pecora, eds., Kluwer, Dordrecht, 2002; (c) S. Hecht, *Functionalizing the interior of dendrimers: synthetic challenges and applications*, *J. Polym. Sci. A* 41 (2003), pp. 1047–1058; (d) G.R. Newkome, C. Moorefield, and F. Vögtle, *Dendrimers and Dendrons*, Wiley-VCH, New York, 2001.
- [12] P.G. de Gennes and H. Hervet, *Statistics of starburst polymers*, *J. Phys. Lett.* 44 (1983), pp. L351–L360.
- [13] S.F. Edwards, *The statistical mechanics of polymers with excluded volume*, *Proc. Phys. Soc. Lond.* 85 (1965), pp. 613–624.
- [14] R.L. Lescanec and M. Muthukumar, *Configurational characteristics and scaling behavior of starburst molecules: a computational study*, *Macromolecules* 23 (1990), pp. 2280–2288.
- [15] D. Boris and M. Rubinstein, *A self-consistent mean field model of a starburst dendrimer: dense core vs dense shell*, *Macromolecules* 29 (1996), pp. 7251–7260; (b) T.C. Zook and G. Pickett, *Hollow-core dendrimers revisited*, *Phys. Rev. Lett.* 90 (2003), 105502.
- [16] R. La Ferla, *Conformations and dynamics of dendrimers and cascade macromolecules*, *J. Chem. Phys.* 106 (1997), pp. 688–700; (b) F. Ganazzoli, R. La Ferla, and G. Terragni, *Conformational properties and intrinsic viscosity of dendrimers under excluded-volume conditions*, *Macromolecules* 33 (2000), pp. 6611–6620; (c) F. Ganazzoli, *Conformations and dynamics of stars and dendrimers: the Gaussian self-consistent approach*, *Condens. Matter Phys.* 5 (2002), pp. 37–71.
- [17] E.G. Timoshenko, Yu.A. Kuznetsov, and R. Connolly, *Conformations of dendrimers in dilute solution*, *J. Chem. Phys.* 117 (2002), pp. 9050–9062.
- [18] M.P. Allen and D.J. Tildesley, *Computer Simulation of Liquids*, Clarendon, Oxford, 1987; D. Frenkel and B. Smit, *Understanding Molecular Simulation*, Academic Press, San Diego, CA, 1996.
- [19] P.K. Maiti, T. Cagin, G. Wang, and W.A. Goddard III, *Structure of PAMAM dendrimers: generations 1 through 11*, *Macromolecules* 37 (2004), pp. 6236–6254.
- [20] F. Tarazona-Vasquez and P.B. Balbuena, *Complexation of the lowest generation poly(amidoamine)-NH<sub>2</sub> dendrimers with metal ions, metal atoms, and Cu(II) hydrates: an ab initio study*, *J. Phys. Chem. B* 108 (2004), pp. 15992–16001; F. Tarazona-Vasquez and P.B. Balbuena, *Ab initio study of the lowest energy conformers and IR spectra of poly(amidoamine)-G0 dendrimers*, *J. Phys. Chem. B* 108 (2004), pp. 15982–15991; Ch. Lin, K. Wu, R. Sa, Ch. Mang, P. Liu, and B. Zhuang, *Density functional theory studies on the potential energy surface and hyperpolarizability of polyamidoamine dendrimer*, *Chem. Phys. Lett.* 363 (2002), pp. 343–348; (d) S.K. Avinash, R.D. Nilesh, and P.G. Shridhar, *Hartree-Fock and density functional studies on the structure and vibrational frequencies of quinoxalines – the building blocks for dendrimers*, *J. Mol. Struct. Theochem.* 589–590 (2002), pp. 301–309.
- [21] (a) R.F.W. Bader, *An Introduction to the Structure of Atoms and Molecules*, Clarke, Toronto, 1970; (b) R.F.W. Bader, *Atoms in Molecules*, Oxford, New York, 1994; (c) P. Ayers, *Atoms in molecules, an axiomatic approach. I. Maximum transferability*, *J. Chem. Phys.* 113 (2000), pp. 10886–10898; (d) R.F.W. Bader and T.T. Nguyen-Dang, *Quantum theory of atoms in molecules: Dalton revisited*, *Adv. Quantum Chem.* 14 (1981), pp. 63–124; (e) A. Cedillo, P.K. Chattaraj, and R.G. Parr, *Atoms-in-molecules partitioning of a molecular density*, *Int. J. Quantum Chem.* 77 (2000), pp. 403–407; (f) F.L. Hirshfeld, *Bonded-atom fragments for describing molecular charge densities*, *Theor. Chim. Acta* 44 (1977), pp. 129–138; (g) R.G. Parr, R.A. Donnelly, M. Levy, and W.E. Palke, *Electronegativity: the density functional viewpoint*, *J. Chem. Phys.* 68 (1978), pp. 3801–3807; (h) R.G. Parr, *Remarks on the concept of an atom in a molecule and on charge transfer between atoms on molecule formation*, *Int. J. Quantum Chem.* 26 (1984), pp. 687–692; (i) J. Rychlewski and R.G. Parr, *The atom in a molecule: a wave function approach*, *J. Chem. Phys.* 84 (1986), pp. 1696–1703; (j) L. Li and R.G. Parr, *The atom in a molecule: a density matrix approach*, *J. Chem. Phys.* 84 (1986), pp. 1704–1711.

- [22] J. Lin, *Divergence measures based on the Shannon entropy*, IEEE Trans. Inf. Theory 37 (1991), pp. 145–151.
- [23] (a) W. Moffitt, *Atoms in molecules and crystals*, Proc. R. Soc. Lond. Ser. A 210 (1951), pp. 245–268; (b) R.S. Mulliken, *Electronic structures of molecules XI. Electroaffinity, molecular orbitals and dipole moments*, J. Chem. Phys. 3 (1935), pp. 573–585; (c) R.S. Mulliken, *Electronic population analysis on LCAOMO molecular wave functions. I*, J. Chem. Phys. 23 (1955), pp. 1833–1840.
- [24] A.E. Reed, R.B. Weinstock, and F. Weinhold, *Natural population analysis*, J. Chem. Phys. 83 (1985), pp. 735–746.
- [25] G. Bruhn, E.R. Davidson, I. Mayer, and A.E. Clark, *Löwdin population analysis with and without rotational invariance*, Int. J. Quantum Chem. 106 (2006), pp. 2065–2072.
- [26] P.O. Löwdin, *Quantum theory of many-particle systems. I. Physical interpretations by means of density matrices, natural spin-orbitals, and convergence problems in the method of configurational interaction*, Phys. Rev. 97 (1955), pp. 1474–1489.
- [27] E. Carrera, N. Flores-Gallegos, and R.O. Esquivel, *Natural atomic probabilities in quantum information theory*, J. Comp. App. Math. DOI : 10.1016/j.cam.2009.02.086.
- [28] (a) S.B. Sears, R.G. Parr, and U. Dinur, *On the quantum-mechanical kinetic energy as a measure of the information in a distribution*, Isr. J. Chem. 19 (1980), pp. 165–173; (b) T. Koga and M. Morita, *Maximum-entropy inference and momentum density approach*, J. Chem. Phys. 79 (1983), pp. 1933–1938; (c) S.R. Gadre, S.B. Sears, S.J. Chakravorty, and R.D. Bendale, *Some novel characteristics of atomic information entropies*, Phys. Rev. A 32 (1985), pp. 2602–2607; (d) J.C. Angulo and J.S. Dehesa, *Tight rigorous bounds to atomic information entropies*, J. Chem. Phys. 97 (1992), pp. 6485–6495; (e) J. Antolín, A. Zarzo, and J.C. Angulo, *Upper and lower bounds on the radial electron density in atoms*, Phys. Rev. A 48 (1993), pp. 4149–4155; (f) J.C. Ramirez, J.M.H. Perez, R.P. Sagar, R.O. Esquivel, M. Ho, and V.H. Smith Jr., *Amount of information present in the one-particle density matrix and the charge density*, Phys. Rev. A 58 (1998), pp. 3507–3515; (g) R.F. Nalewajski and R.G. Parr, *Information theory thermodynamics of molecules and their hirshfeld fragments*, J. Phys. Chem. A 105 (2001), pp. 7391–7400; (h) A. Nagy, *Fisher information in density functional theory*, J. Chem. Phys. 119 (2003), pp. 9401–9405; (i) E. Romera and J.S. Dehesa, *The Fisher–Shannon information plane, an electron correlation tool*, J. Chem. Phys. 120 (2004), pp. 8906–8912; (j) K.D. Sen, *Characteristic features of Shannon information entropy of confined atoms*, J. Chem. Phys. 123 (2005), 074110 (1–9); (k) R.G. Parr, R.F. Nalewajski, and P.W. Ayers, *What is an atom in a molecule?*, J. Phys. Chem. A 109 (2005), pp. 3957–3959; (l) N.L. Guevara, R.P. Sagar, R.O. Esquivel, *Local correlation measures in atomic systems*, J. Chem. Phys. 122 (2005), 084101-1–084101-8; (m) A. Nagy, *Fisher information in a two-electron entangled artificial atom*, Chem. Phys. Lett. 425 (2006), pp. 154–156; (n) W. Ayers, *Density bifunctional theory using the mass density and the charge density*, Theor. Chem. Acc. 115 (2006), pp. 253–256; (o) S.J. Liu, *On the relationship between densities of Shannon entropy and Fisher information for atoms and molecules*, Chem. Phys. 126 (2007), 191107-1–191107-3.
- [29] G. Rudnick and G. Gaspari, *The aspherity of random walks*, J. Phys. A 4 (1986), pp. L191–L194.
- [30] R.G. Parr and R.G. Pearson, *Absolute hardness: Companion parameter to absolute electronegativity*, J. Am. Chem. Soc. 105 (1983), pp. 7512–7516; (b) R.G. Parr, W. Yang, *Density-Functional Theory of Atoms and Molecules*, Oxford University Press, New York, 1989.
- [31] T.A. Koopmans, *Ueber die Zuordnung von Wellenfunktionen und Eigenwerten zu den einzelnen Elektronen eines Atoms*, Physica 1 (1933), pp. 104–113; J.F. Janak, *Proof that  $\partial E/\partial n_i = \epsilon$  in density-functional theory*, Phys. Rev B 18 (1978), pp. 7165–7168.
- [32] T.K. Ghanty and S.K. Ghosh, *Correlation between hardness, polarizability, and size of atoms, molecules, and clusters*, J. Phys. Chem. 97 (1993), pp. 4951–4953; R. Roy, A.K. Chandra, and S. Pal, *Correlation of polarizability, hardness, and electronegativity: polyatomic molecules*, J. Phys. Chem. 98 (1994), pp. 10447–10450; S. Hati and D. Datta, *Hardness and electric dipole polarizability. Atoms and clusters*, J. Phys. Chem. 98 (1994), pp. 10451–10454; Y. Simon-Manso and P. Fuentealba, *On the density functional relationship between static dipole polarizability and global softness*, J. Phys. Chem. A 102 (1998), pp. 2029–2032.
- [33] P.K. Chattaraj, U. Sarkar, and D.R. Roy, *Electrophilicity index*, Chem. Rev. 106 (2006), pp. 2065–2091.
- [34] R.G. Pearson, *Hard and soft acids and bases*, J. Am. Chem. Soc. 85 (1963), pp. 3533–3543; (b) R.G. Pearson, *Hard and Soft Acids and Bases*, Dowen, Hutchinson and Ross, Stroudsburg, 1973; (c) R.G. Pearson, *Chemical Hardness*, Wiley-VCH, New York, 1997.
- [35] R.G. Parr, L.V. Szentpály, and S. Liu, *Electrophilicity index*, J. Am. Chem. Soc. 121 (1999), pp. 1922–1924.
- [36] C.E. Shannon, *A mathematical theory of communication*, Bell Syst. Tech. J. 27 (1948), pp. 379–423.
- [37] I. Bialynicky-Birula and J. Mycielski, *Uncertainty relations for information entropy in wave mechanics*, J. Commun. Math. Phys. 44 (1975), pp. 129–132.
- [38] P.O. Löwdin, *On the orthogonality problem*, Adv. Quantum Chem. 5 (1970), p. 185.
- [39] A.E. Reed and F. Weinhold, *Natural bond orbital analysis of near-Hartree–Fock water dimer*, J. Chem. Phys. 78 (1983), pp. 4066–4073.
- [40] E.R. Davidson, *Electronic population analysis of molecular wavefunctions*, J. Chem. Phys. 46 (1967), pp. 3320–3324.
- [41] (a) A.E. Reed, R.B. Weinstock, and F. Weinhold, *Natural population analysis*, J. Chem. Phys. 83 (1985), pp. 735–746.
- [42] N. Flores-Gallegos and R.O. Esquivel, *von Neumann entropies analysis in Hilbert space for the dissociation processes of homonuclear and heteronuclear diatomic molecules*, J. Mex. Chem. Soc. 52(1) (2008), pp. 19–30.
- [43] A. Wehrl, *General properties of entropy*, Rev. Mod. Phys. 50 (1978), pp. 221–260; V. Vedral, *The role of relative entropy in quantum information theory*, Rev. Mod. Phys. 74 (2002), pp. 197–234.
- [44] C.E. Shannon and W. Weaver, *The Mathematical Theory of Communication*, University of Illinois, Urbana, IL, 1949.
- [45] S. Kullback and R.A. Leibler, *On information and sufficiency*, Ann. Math. Stat. 22 (1951), pp. 79–86.
- [46] E.J. Bylaska, W.A. de Jong, K. Kowalski, T.P. Straatsma, M. Valiev, D. Wang, E. Apra, T.L. Windus, S. Hirata, M.T. Hackler, et al., *NWChem, A Computational Chemistry Package for Parallel Computers, Version 5.0*, Pacific Northwest National Laboratory, Richland, WA, 2006.
- [47] M.J. Frisch, G.W. Trucks, H.B. Schlegel, G.E. Scuseria, M.A. Robb, J.R. Cheeseman, J.A. Montgomery Jr., T. Vreven, K.N. Kudin, J.C. Burant, et al., *Gaussian 03, Revision D.01*, Gaussian, Inc., Wallingford, CT, 2004.
- [48] E.D. Glendening, J.K. Badenhoop, A.E. Reed, J.E. Carpenter, J.A. Bohmann, C.M. Morales, and F. Weinhold, *NBO 5.0*, Theoretical Chemistry Institute, University of Wisconsin, Madison, WI, 2001.
- [49] J.M. Pérez-Jordá and E. San-Fabián, *A simple, efficient and more reliable scheme for automatic numerical integration*, Comput. Phys. Commun. 77 (1993), pp. 46–56; J.M. Pérez-Jordá, A.D. Becke, and E. San-Fabián, *Automatic numerical integration techniques for polyatomic molecules*, J. Chem. Phys. 100 (1994), pp. 6520–6534.
- [50] M. Kohout, *DGRID Program, Version 4.2*, 2007.
- [51] M. Ballauff and C.N. Likos, *Dendrimers in solution: insight from theory and simulation*, Angew. Chem. Int. Ed. 43 (2004), pp. 2998–3020.